Bruschi, Valeria; Välimäki, Vesa; Liski, Juho; Cecchi, Stefania

A Low-Latency Quasi-Linear-Phase Octave Graphic Equalizer

Published in:
Proceedings of the 25th International Conference on Digital Audio Effects (DAFx20in22)

Published: 06/09/2022

Document Version
Publisher's PDF, also known as Version of record

A LOW-LATENCY QUASI-LINEAR-PHASE OCTAVE GRAPHIC EQUALIZER

Valeria Bruschi

Department of Information Engineering
Università Politecnica delle Marche
Ancona, Italy
v.bruschi@staff.univpm.it

Vesa Välimäki

Acoustics Lab, Department of Signal Processing and Acoustics
Aalto University
Espoo, Finland
vesa.valimaki@aalto.fi

Juho Liski

Acoustics Lab, Department of Signal Processing and Acoustics
Aalto University
Espoo, Finland
juho.liski@aalto.fi

Stefania Cecchi

Department of Information Engineering
Università Politecnica delle Marche
Ancona, Italy
s.cecchi@staff.univpm.it

ABSTRACT

This paper proposes a low-latency quasi-linear-phase octave graphic equalizer. The structure is derived from a recent linear-phase graphic equalizer based on interpolated finite impulse response (IFIR) filters. The proposed system reduces the total latency of the previous equalizer by implementing a hybrid structure. An infinite impulse response (IIR) shelving filter is used in the structure to implement the first band of the equalizer, whereas the rest of the band filters are realized with the linear-phase FIR structure. The introduction of the IIR filter causes a nonlinear phase response in the low frequencies, but the total latency is reduced by 50% in comparison to the linear-phase equalizer. The proposed graphic equalizer is useful in real-time audio processing, where only little latency is tolerated.

1. INTRODUCTION

Graphic equalizers (GEQs) are widely used in audio field due to their usability [1, 2, 3]. GEQs have a fixed center frequency, a fixed bandwidth and a variable gain for each band [4] and they are so called because the gain sliders positions define a graph of the magnitude response.

GEQs can be classified as minimum-phase or linear-phase equalizers. The former has the smallest possible latency and does not produce pre-ringing artifacts since the impulse response of the EQ is zero before the main spike, whereas the latter retains the original phase of the signal [5] and does not produce phase distortions that might cause undesired audible effects. For these characteristics, minimum-phase GEQs are highly usable for live music applications where the latency is a key aspect, while linear-phase GEQs are suitable for those applications where the phase response can affect the perception of the audio system such as multichannel equalization [6], speech processing [7], parallel processing, phase compatibility of audio equipment, and crossover network design.

Starting from this classification and focusing on GEQs implementations, minimum-phase equalizers are traditionally developed as a set of infinite impulse response (IIR) filters connected either in cascade [8, 1, 9, 10] or parallel [1, 11, 12, 13]. A recent implementation based on second-order IIR sections (a.k.a. biquads) has been presented in [14, 10, 13] showing good results in terms of accuracy and computational complexity. On the other hand, linear-phase GEQs can be realized by FIR filters [3] that allow for an arbitrary phase response and an implementation that does not suffer from numerical problems, which may require attention in IIR filter implementations [15].

Digital FIR GEQs have existed since the 1980s [16, 17, 18], and similarly to IIR GEQs, the parallel structure is an option [16, 17, 19]. An FIR GEQ can be implemented as a single high-order filter that is used to approximate the target frequency response specified by the user [19]. This operation can be based on the interpolation of the target curve [18, 20], which is not a trivial task due to the fact that the EQ target curve is not well-defined between the command-gain points. Furthermore, the filter length determined by the lowest band could reach several thousand of samples in order to accurately match the target response at low frequencies [18, 21, 22, 23]. Finally, the single FIR may need to be redesigned completely whenever a gain is modified, requiring additional computational effort, which is unsuited for real-time modifications of the target response.

Facing the main problem of the computational complexity reduction, several methods can be found in the literature. For example, frequency-warped FIR filters [24, 25] can be used to shorten the filter lengths especially at low frequencies. However, due to the implementation of the warping function based on IIR transformation, this method produces a non-linear phase response. Another approach is the fast convolution method [26, 27, 28, 29, 30] that is based on fast Fourier transform (FFT) to ensure computational efficiency. In particular, the equalization is obtained applying the inverse Fourier transform to the complex multiplication of the discrete Fourier transforms of the signal and the filter's impulse response. The signal is processed in frames causing much latency, but the FFT-based processing allows for a linear phase response [28].

Aiming at a linear-phase and computational efficient GEQs equalizer, multirate processing can be applied [17, 18, 31, 22]. In this case, the GEQs is realized as a filter bank with different sample rate for each band (i.e., the highest frequency band uses the largest sample rate, whereas the lowest frequency band uses the slowest rate) and, after the filtering, all bands are upsampled back to the

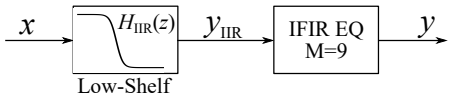

Figure 1: *Scheme of the proposed graphic equalizer.*

original sample rate and summed together.

A different FIR GEQ was proposed by Hergum in [32], where the equalizer is obtained through the application of interpolated FIR filters [33]. Recently, the IFIR theory has been used also in [34] for the implementation of an uniform graphic equalizer. An IFIR filter is composed by the cascade of two FIR filters. The first filter is interpolated by a proper factor producing a periodic frequency response, while the second filter is applied to attenuate the unwanted images [33]. The main advantage of the IFIR filters is that they guarantee a linear phase with a low computational complexity and small ripple. In fact, the implementations of [32, 34] show excellent results with a reduces computational cost, however the audio frequencies are divided in equal bands, contrary to standard GEQs which use a logarithmic band division [3]. For this reason, the approach of [34] has been improved in [35] obtaining a linear-phase octave graphic equalizer based on the IFIR philosophy. In particular, a tree structure built on an FIR lowpass halfband filter is proposed to obtain an octave-band division.

In this paper, a hybrid structure for a quasi-linear-phase graphic equalizer is proposed. The proposed equalizer exploits the existing octave-band structure based on IFIR filters of [35] and introduces an IIR filter to model the first band of the equalizer, in order to reduce the total latency of the system. In particular, the first band is obtained by the design of an eighth order low-shelving filter. Experimental results show that the proposed equalizer reduces the latency by half, maintaining excellent performances in terms of accuracy.

The paper is organized as follows. Section 2 describes the structure of the proposed hybrid graphic equalizer. Section 3 shows the experimental results analyzing the effectiveness of the proposed system. Finally, Section 4 reports the conclusions.

2. PROPOSED EQUALIZER

The proposed octave equalizer has the following ten band center frequencies, or command frequencies: 31.25 Hz, 62.5 Hz, 125 Hz, 250 Hz, 500 Hz, 1.0 kHz, 2.0 kHz, 4.0 kHz, 8.0 kHz, and 16.0 kHz. The bands are numbered from lowest to highest using index $m = 1, 2, 3, ..., 10$ and each mth band presents a desired dB-gain $\Gamma_m = 20\log_{10}(g_m)$, chosen by the user. A sample rate of $f_s = 48$ kHz has been used in this design.

The scheme of the proposed equalizer is shown in Fig. 1. The total structure is obtained combining IIR and FIR filters. In particular, the input signal $x(n)$ is filtered by an eighth-order IIR low-shelving filter that designs the first band of the GEQ. Then, the output of the IIR part $y_{IIR}(n)$ is filtered by the IFIR filterbank that implements $M = 9$ bands, from the second to the tenth, using our recently proposed structure [35].

2 shows the magnitude response of the IIR filter $H_{IIR}(z)$, of the IFIR filterbank with $M = 9$ and of the total equalizer with a zigzag command setting (± 12 dB). In the figure, the red circles correspond to the desired gain of each mth band g_m at the related center frequency. The design of the IIR filter and of the IFIR filterbank is explained below.

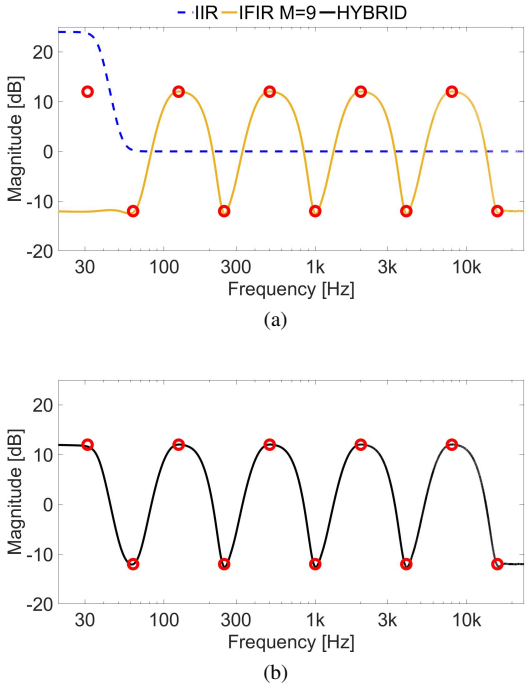

Figure 2: *Magnitude responses of (a) the IIR part of the equalizer and the IFIR part and (b) the total proposed hybrid equalizer after the gains computation with the zigzag configuration (± 12 dB).*

2.1. IIR equalizer

The first band of the equalizer is obtained through a 8th-order lowpass IIR shelving filter, that is designed following the implementation of [36]. The order of the IIR filter is defined as $P = 8$ and the gain is set to

$$\Gamma = \Gamma_1 - \Gamma_2, \tag{1}$$

where Γ_1 and Γ_2 are the desired dB-gains of the first and the second band, respectively. The gain of the second band is subtracted to restore the low-frequencies gains to zero, since the second band is designed as a lowpass filter in the IFIR structure. The linear value of the IIR filter gain is defined as $g = 10^{\Gamma/20}$.

In this paper, for the design of the shelving filter, the normalized digital cutoff frequency is set to the geometric mean of the neighboring center frequencies, that is,

$$\Omega_C = \sqrt{\Omega_U \Omega_L}, \tag{2}$$

where $\Omega_L = 2\pi \cdot 31.25/f_s$ and $\Omega_U = 2\pi \cdot 62.5/f_s$, respectively. This results in a cutoff frequency in Hertz of approximately 44 Hz that corresponds to the center point between the two first center frequencies on a logarithmic axis. The transfer function of the low-shelving IIR filter $H_{IIR}(z)$ comprises cascade second-order sections, and it is obtained as

$$H_{IIR}(z) = \prod_{i=1}^{P/2} \left(1 + 2V \frac{K\left(K + c_i + 2Kz^{-1} + (K - c_i)z^{-2}\right)}{1 + 2Kc_i + K^2 + (2K^2 - 2)z^{-1} + (1 - 2Kc_i + K^2)z^{-2}} + V^2 \frac{K^2\left(1 + 2z^{-1} + z^{-2}\right)}{1 + 2Kc_i + K^2 + (2K^2 - 2)z^{-1} + (1 - 2Kc_i + K^2)z^{-2}}\right), \tag{3}$$

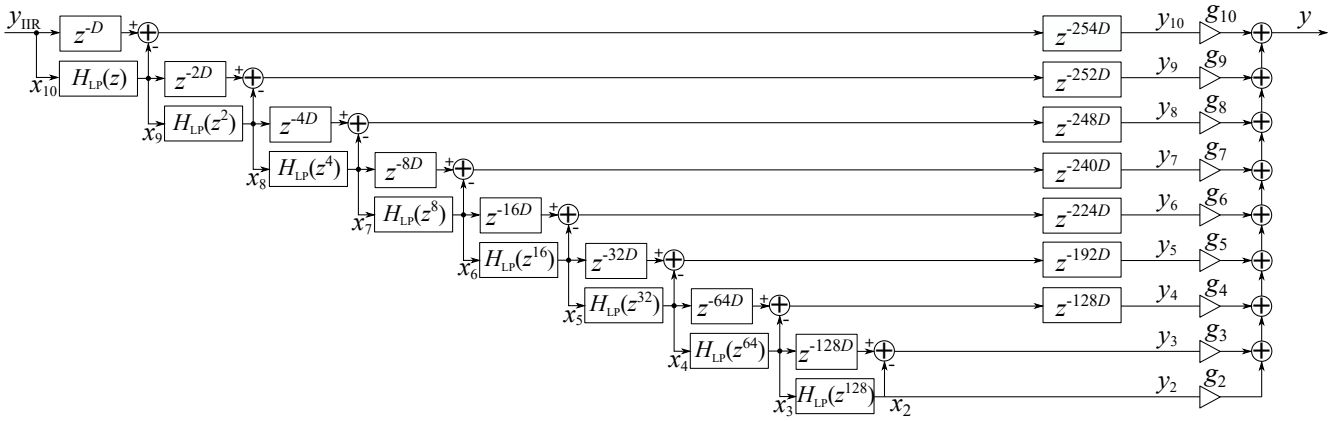

Figure 3: *IFIR GEQ structure implementing the bands from the second to the tenth is a modification of a previous 10-band GEQ [35].*

where $V = \sqrt[P]{g} - 1$ and $c_i = \cos(\alpha_i)$, with

$$\alpha_i = \left(\frac{1}{2} - \frac{2i-1}{2P}\right)\pi. \tag{4}$$

Looking at Equation (3), the three terms of the product describe a unique second-order section, since the denominators of the second-order terms are identical. The constant K is used to map the desired digital cutoff frequency Ω_C to the analog one $\omega_C = \sqrt[2P]{g}$ and it is computed as

$$K = \frac{1}{\sqrt[2P]{g}} \tan\left(\frac{\Omega_C}{2}\right). \tag{5}$$

The magnitude frequency response of the 8th-order low-shelving filter is shown by the blue curve of Fig. 2(a). In this case a zigzag configuration with ± 12 dB is applied, so the gain Γ of the IIR filter is set to 24 dB (12 + 12 dB), according to Equation (1).

Once the IIR filter is designed, the output signal of the IIR equalizer $y_{IIR}(n)$ is obtained by filtering the input signal $x(n)$ with the obtained filter as shown in Fig. 1, so the Z transform of the output $Y_{IIR}(z)$ is obtained as follows:

$$Y_{IIR}(z) = H_{IIR}(z)X(z). \tag{6}$$

2.2. IFIR equalizer

The signal filtered by the IIR filter $y_{IIR}(n)$ is used as input to the IFIR equalizer, as shown in Fig. 1. The IFIR structure of [35] is used in the proposed system to design the nine bands from the second to the tenth. The scheme of the IFIR equalizer is shown in Fig. 3. A tree structure with subtraction is implemented to obtain a perfect reconstruction filterbank. The tree structure is derived from a halfband lowpass prototype FIR filter $H_{LP}(z)$ with cutoff frequency of 12 kHz, which is half of the Nyquist limit 24 kHz. The filter $H_{LP}(z)$ is designed with the Kaiser window, imposing an order of $N = 18$ and a parameter $\beta = 4$ [37]. The advantage of the halfband filter is the fact that one every second sample of the impulse response is zero by definition, except for the middle coefficient [38]. In this way the computational cost can be reduced considering only the non-zero elements of the impulse response, calculated as $N_{nz} = N/2+2$. The nine bands of the IFIR equalizer are numbered from the lowest to the highest using the index $m = 2, 3, ..., M+1$, with $M = 9$.

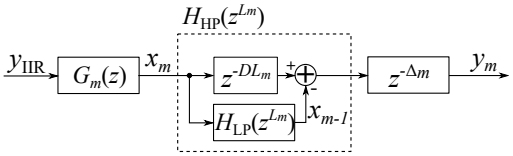

Figure 4: *Filters and delay lines associated with a single band for $m = 3, 4, ..., M+1$ with $M = 9$, cf. Fig. 3. This mth band transfer function $H_m(z)$ represents the relation between $Y_m(z)$ and $Y_{IIR}(z)$.*

The highest band of the equalizer $H_{10}(z)$ is designed as a complementary highpass filter of the prototype filter as

$$H_{10}(z) = z^{-D} - H_{LP}(z), \tag{7}$$

where the delay is computed as $D = N/2$. According to Equation (7), the filter $H_{HP}(z)$ can be implemented using a delay line and a subtraction, once the lowpass filtered signal going to the lower bands has been computed using $H_{LP}(z)$, as shown in the top right corner of Fig. 3.

The rest of the bands of the filterbank are obtained with stretched versions of the prototype filter, such as $H_{LP}(z^2)$ and $H_{LP}(z^4)$, which are prepared by inserting one or three zero samples between each two coefficients of the prototype FIR filter, respectively [38]. The general scheme of delay and filtering operations for the mth band is presented in Fig. 4. The Z transform of the mth band output signal $Y_m(z)$ is obtained from the signal $Y_{IIR}(z)$ as follows:

$$Y_m(z) = H_m(z)Y_{IIR}(z), \tag{8}$$

where $H_m(z)$ is the transfer function of the mth band and is com-

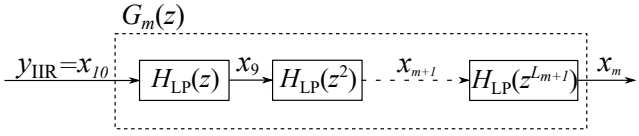

Figure 5: *Details of the transfer function $G_m(z)$ used in Fig. 4.*

puted as

$$H_m(z) = z^{-\Delta_m}[z^{-DL_m} - H_{\text{LP}}(z^{L_m})]G_m(z), \quad (9)$$

where the mth interpolation factor L_m is computed as

$$L_m = 2^{(M-m+1)} = 2^{(10-m)}, \quad (10)$$

and $G_m(z)$ represents the interpolation filter of the mth band. In the proposed approach, the simple interpolation filter described in [33] is replaced by the cascade of the existing lowpass filters of the tree structure, as shown in Fig. 5, i.e.,

$$G_m(z) = H_{\text{LP}}(z) \prod_{k=m+1}^{M} H_{\text{LP}}(z^{L_k}), \quad (11)$$

with $m = 3, ..., M+1$ and $M = 9$.

Looking at Fig. 4, the input signal $y_{\text{IIR}}(n)$ is first filtered by the filter $G_m(z)$ and the resulting intermediate signal $x_m(n)$, shown for each band in Fig. 3, is then filtered by $H_{\text{HP}}(z^{L_m})$ that is implemented through a delay line and a subtraction, according to Equation (7). Note that in Fig. 4, when $m = 9$, the signal $x_{10}(n)$ corresponds to the input signal $y_{\text{IIR}}(n)$, which is also seen in the top left corner in Fig. 3.

To better understand the design of each band of the IFIR filterbank, Fig. 6 shows a design example of the fifth band, with a center frequency of 500 Hz. The transfer function of the sixth band $H_5(z)$ is obtained by the concatenation of the filter $G_5(z)$ and the filter $H_{\text{HP}}(z^{L_5}) = z^{-DL_5} - H_{\text{LP}}(z^{L_5})$, according to Equation (9).

A synchronization delay Δ_m, also shown in Fig. 4, must be applied in order to align all the band outputs, and is determined as

$$\Delta_m = \tau - [2^{(M+2-m)} - 1]D = \tau - [2^{(11-m)} - 1]D, \quad (12)$$

where τ is the total delay of the equalizer in samples:

$$\tau = [2^{(M-1)} - 1]D = 255D. \quad (13)$$

In Fig. 3, the synchronization delays Δ_m are shown one upon the other on the right-hand side, next to the command gain factors g_m. In the highest band (the top signal path in Fig. 3), the total delay of $255D$ samples is formed by the cascade of the delay line z^{-D} and the synchronization delay z^{-254D}. In the second band (the lowest of the IFIR equalizer), the synchronization delay is formed by the cascade of all the delay lines between the input (top left corner in Fig. 3) and the output y_2 (bottom right corner in Fig. 3), which have the lengths D, $2D$, $4D$, $8D$, $16D$, $32D$, $64D$ and $128D$. This adds up to $255D$ samples of delay.

The second band filter of the equalizer is obtained as a byproduct, when the signal $x_3(n)$ is filtered with the prototype filter stretched by a factor of 2^7, or 128, as shown in Fig. 3. The resulting signal $x_2(n)$ does not require further processing, as it is the output signal $y_2(n)$ of the second band filter. The filter $H_{\text{LP}}(z^{128})$ also implements the largest input-output delay, so a synchronization delay is unnecessary in the two lowest bands, as seen in Fig. 3.

Finally, as presented in Fig. 3, gain factor g_m of each band is applied and the total response of the equalizer $y(n)$ is obtained as a weighted sum of all band output signals from the second band to the tenth:

$$y(n) = \sum_{m=2}^{M+1} g_m y_m(n). \quad (14)$$

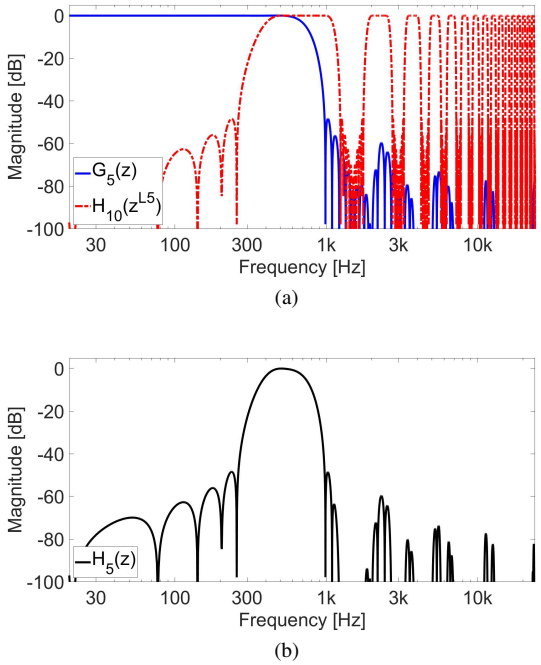

Figure 6: *Example of the design of the magnitude response of the band filter centered at 500 Hz. Cascading the filters (a) $G_5(z)$ and $H_{HP}(z^{L_5}) = z^{-DL_5} - H_{LP}(z^{L_5})$ results in (b) the band filter $H_5(z)$.*

An example of the magnitude response of the IFIR equalizer is shown by the yellow curve of Fig. 2, where a zigzag configuration of command setting is applied with ± 12 dB. The IFIR magnitude response is the same of the response of the total hybrid equalizer except in the first band, since the IFIR part affects the overall equalizer from the second to the tenth band. The low-frequency part of the IFIR output maintains the same gain of the second band filter, since it is designed as a lowpass filter.

3. EXPERIMENTAL RESULTS

In the experiments, the proposed hybrid IIR/FIR equalizer is compared with the IFIR equalizer of [35] in terms of latency, computational complexity and error. Table 1 shows the obtained results. The latency is introduced only by the FIR part of the equalizer and it is computed as shown by Equation (13). In the proposed equalizer, only the last nine bands are designed with FIR filters, so the total delay is $255D$. On the contrary, in the linear-phase equalizer of [35], all the ten band are designed with FIR filters (i.e., $M = 10$) and the resulting delay is doubled obtaining a value of $511D$.

The computational complexity is evaluated in terms of number of multiplications and number of additions per input sample. The filtering with the IFIR filterbank is achieved by avoiding multiplications with zero elements, so only the number of non-zero elements N_{nz} is involved. Taking into account also the symmetry of the FIR impulse responses, the number of multiplications of the

Table 1: *Performance of the proposed hybrid equalizer compared with the IFIR-based GEQ. The symmetry has been accounted for in the number of multiplications. The best result for each column is highlighted.*

Method	Latency	Mul	Add	Error [dB]
IFIR GEQ [35]	4599	**64**	**108**	0.79
Hybrid GEQ (proposed)	**2295**	77	112	**0.76**

FIR part is computed as

$$\text{n}^\circ \text{ mult. (FIR)} = (M-1)\frac{N_{\text{nz}}+1}{2} + M. \tag{15}$$

Finally, the number of additions is calculated as follows:

$$\text{n}^\circ \text{ add. (FIR)} = (M-1)N_{\text{nz}} + M - 1. \tag{16}$$

For the proposed equalizer, the computational complexity of the FIR part is obtained with $M = 9$, while the 8th-order shelving IIR filter adds $5P/2 = 20$ multiplications and $4P/2 = 16$ additions to the total number of operations, considering a cascade of four (corresponding to P/2) second-order sections implemented with the direct form II.

The error in the frequency response is calculated as the maximum difference between the desired and the obtained gains at the octave center frequencies, including all the possible configurations with ± 12 dB, which leads to 1024 cases in total [39]. Moreover, when two adjacent bands have the same gain, the error is computed as the maximum deviation from the straight line that connects the two gains at the center frequencies. Previous publications, as [36, 39], consider the error as acceptable when it is below 1 dB and listening tests in [40, 41] have proven that just noticeable difference in the deviation of the magnitude response is higher than ± 1 dB for most of the input signals, as stated also in [42].

The results show the latency of the proposed equalizer is reduced by 50% in comparison with the IFIR equalizer of [35]. In fact, the FIR equalizer introduces a latency of 4599 samples (or 96 ms with a sampling frequency of 48 kHz), while the proposed hybrid equalizer shows a latency of only 2295 samples (or 48 ms). This reduction allows the equalizer to be more competitive in real-time applications, where a big latency is not tolerated. The computational complexity of the hybrid equalizer is a bit higher than the IFIR equalizer. In fact, the IFIR equalizer needs a total of 172 operations per input sample (64 multiplications and 108 additions), while the proposed method needs 189 operations (77 multiplications and 112 additions).

Finally, the error of the proposed equalizer is 0.76 dB and is slightly lower than the error introduced by the IFIR equalizer, so it is still less than the acceptable limit of ± 1 dB. Fig. 7 shows example magnitude frequency responses of three different test configurations:

a) the zigzag command settings (± 12 dB);

b) the special zigzag setting: [12 -12 -12 12 -12 -12 12 -12 -12 12] dB, which is declared the most difficult case for the equalizer of [43];

c) an arbitrary setting: [8 10 -9 10 3 -10 -6 1 11 12] dB.

As can be seen in Fig. 7, the magnitude response of the proposed equalizer perfectly overlaps the response of the IFIR equalizer except in the transition of the first band, where the shelving filter is applied. In fact, in the proposed equalizer, the first band is narrower than the first band of the IFIR EQ. However, this characteristic does not affect the performance of the final GEQ, since the desired gain at the first center frequency is always reached.

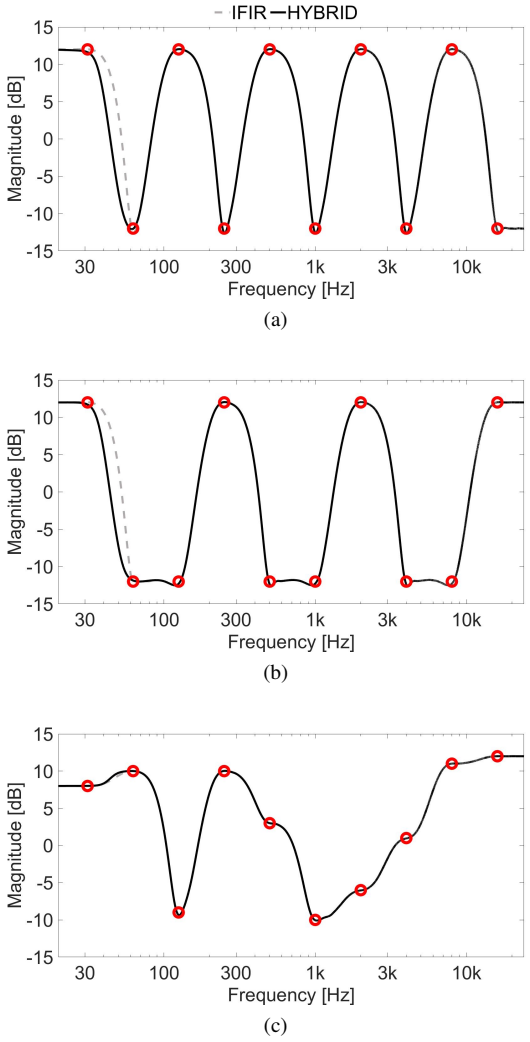

Figure 7: *Magnitude response of the proposed hybrid equalizer compared with the total IFIR equalizer, with (a) the zigzag configuration (± 12 dB), (b) the gains [12 -12 -12 12 -12 -12 12 -12 -12 12] dB, and (c) the arbitrary gains [8 10 -9 10 3 -10 -6 1 11 12] dB.*

Figure 8 shows the total impulse response of the proposed equalizer compared with the IFIR equalizer. This comparison highlights that the nonlinear-phase IIR filters barely affect the symmetry of the total impulse response, but allow to reduce the delay by half.

The latency reduction introduced by the proposed equalizer is shown also in 9, where the group delays of the two implementations are compared. The IFIR equalizer presents a constant group delay of 95.8 ms that means it has a linear phase. The proposed equalizer introduces a nonlinearity in the phase at the lower frequencies up to 100 Hz, but at higher frequencies the group delay assumes a constant value of 47.8 ms.

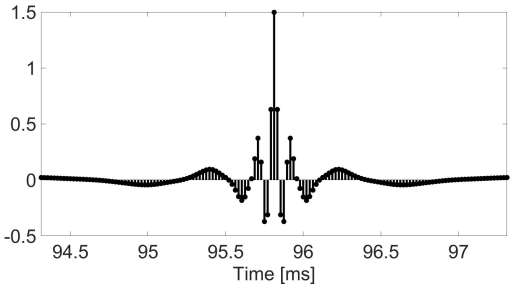

(a)

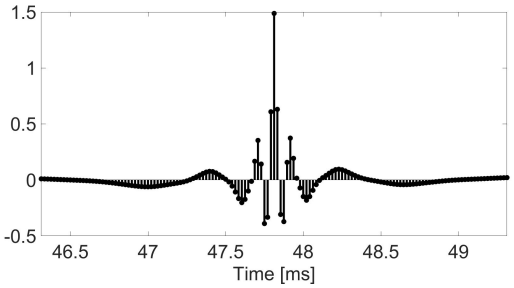

(b)

Figure 8: *Impulse response (a) of the linear-phase IFIR equalizer of [35] and (b) of proposed equalizer with the configuration of Fig. 7(a), which is slightly asymmetric.*

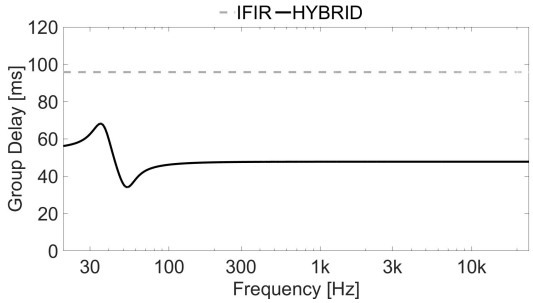

Figure 9: *Comparison of group delay functions of the proposed equalizer with the configuration of Fig. 7(a) and the linear-phase IFIR equalizer of [35]. The curves show that the proposed method reduces the latency by 50% at frequencies above about 100 Hz.*

4. CONCLUSION

This paper proposes a low-latency quasi-linear-phase octave graphic equalizer. The proposed structure reduces the total latency of an existing linear-phase graphic equalizer by replacing its lowest band filter with an IIR filter. The first band of the equalizer is designed as an IIR shelving filter of order 8. The performance of the equalizer has been evaluated in comparison with the linear-phase IFIR GEQ in terms of latency, computational complexity, and accuracy.

The experimental results given in this paper show that the proposed GEQ reduces the latency by 50%, so that it is now less than 50 ms. The nonlinear phase response at the low frequencies has a minor effect on the impulse-response symmetry of the proposed GEQ. The approximation error is also slightly reduced, which means that the proposed GEQ is more accurate than the IFIR-based GEQ. The computational complexity is slightly increased while is still comparable with the one of the IFIR equalizer. This paper shows that it is practical to demand linear-phase processing at most of the audio range and still reach a latency that is not too large in practice.

5. ACKNOWLEDGMENTS

This research was initiated when the first author was a visitor at the Aalto Acoustics Lab from September to December 2021. This work is part of the activities of the Nordic Sound and Music Computing Network—NordicSMC (NordForsk project no. 86892). Part of this work is supported by Marche Region in implementation of the financial programme POR MARCHE FESR 2014-2020, project "Miracle" (Marche Innovation and Research fAcilities for Connected and sustainable Living Environments), CUP B28I19000330007.

6. REFERENCES

[1] Richard A. Greiner and Michael Schoessow, "Design aspects of graphic equalizers," *J. Audio Eng. Soc.*, vol. 31, no. 6, pp. 394–407, Jun. 1983.

[2] S. K. Mitra and J. F. Kaiser, *Handbook for Digital Signal Processing*, John Wiley & Sons, New York, NY, USA, 1st edition, Aug. 1993.

[3] V. Välimäki and J. D. Reiss, "All about audio equalization: Solutions and frontiers," *Appl. Sci.*, vol. 6, no. 5, May 2016.

[4] Dennis A Bohn, "Constant-Q graphic equalizers," *J. Audio Eng. Soc.*, vol. 34, no. 9, pp. 611–626, Sep. 1986.

[5] Alexis Favrot and Christof Faller, "Wiener-based spatial B-format equalization," *J. Audio Eng. Soc.*, vol. 68, no. 7/8, pp. 488–494, Jul./Aug. 2020.

[6] J. Vilkamo, T. Bäckström, and A. Kuntz, "Optimized covariance domain framework for time–frequency processing of spatial audio," *J. Audio Eng. Soc.*, vol. 61, no. 6, pp. 403–411, Jun. 2013.

[7] B. D. Radlovic and R. A. Kennedy, "Nonminimum-phase equalization and its subjective importance in room acoustics," *IEEE Trans. Speech Audio Process.*, vol. 8, no. 6, pp. 728–737, Nov. 2000.

[8] Y. Hirata, "Digitalization of conventional analog filters for recording use," *J. Audio Eng. Soc.*, vol. 29, no. 5, pp. 333–337, May 1981.

[9] S. Prince and K. R. S. Kumar, "A novel *N*th-order IIR filter-based graphic equalizer optimized through genetic algorithm for computing filter order," *Soft Comput.*, vol. 23, no. 8, pp. 2683–2691, Apr. 2019.

[10] J. Rämö, J. Liski, and V. Välimäki, "Third-octave and bark graphic-equalizer design with symmetric band filters," *Appl. Sci.*, vol. 10, no. 4, pp. 1–22, Feb. 2020.

[11] S. Tassart, "Graphical equalization using interpolated filter banks," *J. Audio Eng. Soc.*, vol. 61, no. 5, pp. 263–279, May 2013.

[12] J. Rämö, V. Välimäki, and B. Bank, "High-precision parallel graphic equalizer," *IEEE/ACM Trans. Audio Speech Lang. Process.*, vol. 22, no. 12, pp. 1894–1904, Dec. 2014.

[13] J. Liski, B. Bank, J. O. Smith, and V. Välimäki, "Converting series biquad filters into delayed parallel form: Application to graphic equalizers," *IEEE Trans. Signal Process.*, vol. 67, no. 14, pp. 3785–3795, Jul. 2019.

[14] V. Välimäki and J. Liski, "Accurate cascade graphic equalizer," *IEEE Signal Process. Lett.*, vol. 24, no. 2, pp. 176–180, Feb. 2017.

[15] K. Horváth and B. Bank, "Optimizing the numerical noise of parallel second-order filters in fixed-point arithmetic," *J. Audio Eng. Soc.*, vol. 67, no. 10, pp. 763–771, Oct. 2019.

[16] J. A. Jensen, "A new principle for an all-digital preamplifier and equalizer," *J. Audio Eng. Soc.*, vol. 35, no. 12, pp. 994–1003, Dec. 1987.

[17] J. Henriquez, T. Riemer, and R. Trahan Jr., "A phase-linear audio equalizer: Design and implementation," *J. Audio Eng. Soc.*, vol. 38, no. 9, pp. 653–666, Sept. 1990.

[18] M. Waters, M. Sandler, and A. C. Davies, "Low-order FIR filters for audio equalization," in *Proc. 91st Convention of the Audio Engineering Society*, Oct. 1991, paper 3188.

[19] D. S. McGrath, "An efficient 30-band graphic equalizer implementation for a low-cost DSP processor," in *Proc. 95th Convention of the Audio Engineering Society*, Oct. 1993, paper 3756.

[20] Paul H. Kraght, "A linear-phase digital equalizer with cubic-spline frequency response," *J. Audio Eng. Soc.*, vol. 40, no. 5, pp. 403–414, May 1992.

[21] D. S. McGrath, "A new approach to digital audio equalization," in *Proc. 97th Convention of the Audio Engineering Society*, San Francisco, CA, Nov. 1994, paper 3899.

[22] R. Väänänen and J. Hiipakka, "Efficient audio equalization using multirate processing," *J. Audio Eng. Soc.*, vol. 56, no. 4, pp. 255–266, Apr. 2008.

[23] M. K. Othman and T. H. Lim, "Run time analysis of an audio graphic equalizer for portable industrial directional sound systems in industrial usage," in *Proceedings of the 14th IEEE Conference on Industrial Electronics and Applications (ICIEA)*, Xi'an, China, Jun. 2019, pp. 2177–2181.

[24] R. J. Oliver, "Frequency-warped audio equalizer," US Patent 7,764,802 B2, Jul. 2010.

[25] J. Siiskonen, "Graphic Equalization Using Frequency-Warped Digital Filters," Master's thesis, Aalto University School of Electrical Engineering, Espoo, Finland, Jul. 2016, `https://aaltodoc.aalto.fi/handle/123456789/21593`.

[26] T. G. Stockham Jr., "High-speed convolution and correlation," in *Proceedings of the Spring Joint Computer Conference*, New York, NY, Apr. 1966, vol. 28, pp. 229–233.

[27] Barry D. Kulp, "Digital equalization using Fourier transform techniques," in *Proc. 85th Convention of the Audio Engineering Society*, Los Angeles, CA, Oct. 1988, paper 2694.

[28] H. Schöpp and H. Hetze, "A linear-phase 512-band graphic equalizer using the fast-Fourier transform," in *Proc. 6th Convention of the Audio Engineering Society*, Feb. 1994, paper 3816.

[29] G. F. P. Fernandes, L. G. P. M. Martins, M. F. M. Sousa, F. S. Pinto, and A. J. S. Ferreira, "Implementation of a new method to digital audio equalization," in *Proc. 106th Convention of the Audio Engineering Society*, Munich, Germany, May 1999, paper 4895.

[30] S. Ries and G. Frieling, "PC-based equalizer with variable gain and delay in 31 frequency bands," in *Proc. 108th Convention of the Audio Engineering Society*, Paris, France, Feb. 2000, paper 5173.

[31] S. Cecchi, L. Palestini, E. Moretti, and F. Piazza, "A new approach to digital audio equalization," in *Proceedings of the IEEE Workshop on Applications of Signal Processing to Audio and Acoustics (WASPAA)*, New Paltz, NY, Oct. 2007, pp. 62–65.

[32] R. Hergum, "A low complexity, linear phase graphic equalizer," in *Proc. 85th Convention of the Audio Engineering Society*, Nov. 1988, paper 2738.

[33] Y. Neuvo, D. Cheng-Yu, and S. Mitra, "Interpolated finite impulse response filters," *IEEE Trans. Acoust. Speech Signal Process.*, vol. 32, no. 3, pp. 563–570, Jun. 1984.

[34] Valeria Bruschi, Stefano Nobili, Alessandro Terenzi, and Stefania Cecchi, "A low-complexity linear-phase graphic audio equalizer based on IFIR filters," *IEEE Signal Process. Lett.*, vol. 28, pp. 429–433, Feb. 2021.

[35] V. Bruschi, V. Välimäki, J. Liski, and S. Cecchi, "Linear-phase octave graphic equalizer," *J. Audio Eng. Soc.*, vol. 70, no. 6, pp. 435–445, June 2022, Special Issue on Audio Filter Design.

[36] M. Holters and U. Zölzer, "Graphic equalizer design using higher-order recursive filters," in *Proceedings of the International Conference on Digital Audio Effects (DAFx)*, Montreal, Canada, Sep. 2006, pp. 37–40.

[37] A. V. Oppenheim and R. W. Schafer, *Discrete-Time Signal Processing*, Prentice-Hall, Inc., Upper Saddle River, NJ, 1999, Chapter 7, pp. 465-478.

[38] P. P. Vaidyanathan, *Multirate Systems and Filterbanks*, Prentice-Hall, Inc., Englewood Cliffs, NJ, 1993, Chapter 4, pp. 134-143.

[39] J. Liski and V. Välimäki, "The quest for the best graphic equalizer," in *Proceedings of the 20th International Conference on Digital Audio Effects (DAFx)*, Edinburgh, UK, Sep. 2017, pp. 95–102.

[40] Floyd E. Toole and Sean E. Olive, "The modification of timbre by resonances: Perception and measurement," *J. Audio Eng. Soc.*, vol. 36, no. 3, pp. 122–142, Mar. 1988.

[41] Louis D. Fielder, "Analysis of traditional and reverberation-reducing methods of room equalization," *J. Audio Eng. Soc.*, vol. 51, no. 1/2, pp. 3–26, Feb. 2003.

[42] Henri Korhola and Matti Karjalainen, "Perceptual study and auditory analysis on digital crossover filters," *J. Audio Eng. Soc.*, vol. 57, no. 6, pp. 413–429, Jun. 2009.

[43] Richard J. Oliver and Jean-Marc Jot, "Efficient multi-band digital audio graphic equalizer with accurate frequency response control," in *Proc. 139th Convention of the Audio Engineering Society*, Oct. 2015, paper 9406.